AIP | Applied Physics Letters

Room temperature persistent photoconductivity in p-PbTe and p-PbTe:BaF2

S. de Castro, D. A. W. Soares, M. L. Peres, P. H. O. Rappl, and E. Abramof

Citation: Applied Physics Letters **105**, 162105 (2014); doi: 10.1063/1.4899140
View online: http://dx.doi.org/10.1063/1.4899140
View Table of Contents: http://scitation.aip.org/content/aip/journal/apl/105/16?ver=pdfcov
Published by the AIP Publishing

Room temperature persistent photoconductivity in *p*-PbTe and *p*-PbTe:BaF_2

S. de Castro,[1,a)] D. A. W. Soares,[1] M. L. Peres,[1] P. H. O. Rappl,[2] and E. Abramof[2]
[1]*Departamento de Física e Química, Universidade Federal de Itajubá, Itajubá, PB 50, MG CEP 37500-903, Brazil*
[2]*Laboratório Associado de Sensores e Materiais, Instituto Nacional de Pesquisas Espaciais, São José dos Campos, PB 515, SP CEP 12201-970, Brazil*

(Received 1 September 2014; accepted 11 October 2014; published online 23 October 2014)

We investigated the persistent photoconductivity effect observed in *p*-PbTe:BaF_2 and undoped *p*-PbTe films in the temperature range of $T = 100$–300 K. It was observed that the PPC effect scales with temperature and that there is a transition in the relaxation time behavior around ~150 K. We found that the transition is caused by the particular dynamics of the hole carries between the energy barriers that characterize the traps originated from disorder present in the samples. The analysis was performed by comparing the theory of the random potential with the experimental data and revealed the presence of both random local potential fluctuations and localized states, which can be attributed to the presence of disorder due BaF_2 doping and Te vacancies. © *2014 AIP Publishing LLC*. [http://dx.doi.org/10.1063/1.4899140]

Persistent photoconductivity (PPC) has been observed in different materials and the origin of this effect is attributed to several reasons including the formation of points defects, as DX centers,[1,2] metastable defects,[3] and presence of local potential fluctuation.[4] Each system can present one or more of these mechanisms and a detailed analysis is often required in order to identify each mechanism. The investigation of such effect can reveal the presence of impurity levels and help to improve the performance of optoelectronic devices.[5–7] More recently, it was proposed that the PPC can be used for the development of holographic memories.[8] However, some issues must be overcome in order to develop a functional device such as the observation of PPC effect at room temperature and the reduction of electronic noise.

The PPC effect occurs due to light induced change in free carrier concentration, which persists for a long period of time after illumination is removed. So far, room temperature PPC has been observed in wide gap semiconductors such as $SrTiO_3$,[8] Cu_2ZnSnS_4 (CZTS),[4] and Zn_3P_2.[3] PbTe films that present insulating behavior, such as *n*-PbTe doped with Ga[9] and undoped *p*-PbTe,[10] exhibits PPC at low temperatures ($T < 77$ K) when they are illuminated with GaAs light-emitting diode (LED). Surprisingly, *p*-PbTe films investigated in this work showed remarkable photosensitivity response at room temperature, even in the metallic regime, and presented strong PPC effect characterized by long recombination times.

PbTe is known as a narrow gap semiconductor and its study has been motivated over several decades due its extraordinary physical properties and its importance in infrared diodes,[11] thermoelectric devices,[12] and detectors.[13] PbTe based structures can present high carrier mobility and its Fermi surface consists of four equivalent ellipsoids of rotation with axis along the ⟨111⟩ direction at the *L* point of the Brillouin zone.[14] The physics is further enriched by the large value of the Landé *g* factor and the small effective mass; both of which display considerable anisotropy. In addition, the strong spin-orbit coupling presented in PbTe films and quantum wells make PbTe an interesting material for possible applications in spintronics.[15] In the present work, we studied undoped non-stoichiometric *p*-PbTe and *p*-PbTe:BaF_2 samples that exhibit persistent photoconductivity at room temperature and the investigation was carried to low temperatures where the effect vanishes.

The *p*-PbTe:BaF_2 film was studied for temperatures ranging from room temperature down to liquid nitrogen temperature. It was found that the effect of PPC is strongly temperature dependent and is suppressed for regions close to 100 K. To explain the PPC effect observed in the experimental measurements, we used the Random Potential model to calculate the size of the energy barriers caused by the disorder.[16] The calculated values are very close to those obtained from experimental data. With this analysis, it was found that there are two barriers involved in these photoconductivity processes: one due to the intrinsic disorder present in PbTe and the other created by doping the samples with BaF_2. The experimental results indicate that there is an energy barrier that is not at *L* point of the Brillouin zone, suggesting that the hole trapping by this barrier is phonon assisted. The recombination times found were the order of hours, reaching a maximum value of ~80 h, revealing the potential application of these materials for the development of holographic memory devices.

For the electrical transport measurements, pieces of non-stoichiometric *p*-PbTe undoped and *p*-PbTe:BaF_2 with doping temperature (T_D) ~ 650 °C (doping level <0.01%) were used. They were contacted in approximate Van der Pauw geometry by soldering Au wires with In pellets. A comprehensive description of the sample growth procedure is given in Ref. 17. The samples investigated were cooled in a closed cryostat from 300 K down to 77 K and illuminated by a blue LED under vacuum conditions. Some basic transport characteristics for the investigated samples, obtained via Van-der-Pauw technique, are presented in Table I.

Figure 1 shows the time dependence of the photoconductivity normalized (σ_N) buildup and decay at 300 K for

a)Author to whom correspondence should be addressed. Electronic mail: suelenfisica@yahoo.com.br

TABLE I. BaF_2 doping temperature (T_D) of the *p*-PbTe samples and their corresponding hole concentrations (p), Hall mobilities (μ), and resistivity (ρ) at 300 K.

T_D (°C)	p (10^{23} m^{-3})	μ (10^{-2} m^2/V s)	ρ (10^{-4} Ω·m)	Thickness (μm)
650	4.2	2.3	6.6	3.5
[a]	5.1	3.7	3.34	2.8

[a]Undoped *p*-PbTe sample.

p-PbTe and *p*-PbTe:BaF_2 samples under illumination by blue LED at normal incidence. The normalized photoconductivity presents an increase for both samples during illumination indicating that the density of the holes in the valence band also increases during illumination.[18] Once the light is turned off, the samples photoconductivity does not immediately recover to its original states, but decreases slowly, exhibiting the persistent conductivity effect. This effect has already been observed by other research groups at room temperature but, differently from our samples, only in insulating materials.[3,8,9,19] We suggest that the slow decrease of the dark conductivity can be attributed to the interaction of impurity centers with the lattice that modifies the potential of impurity atoms and produces deep levels in the energy spectrum[20] of the crystal structure. Such impurities can have two origins: The disorder produced during the non stoichiometric growth of the samples and the disorder caused by the BaF_2 doping.

The decay of the photoconductivity observed in the investigated samples shows approximately the exponential behavior given by

$$\sigma(t) = \sigma_0 \exp\left(-\frac{t}{\tau}\right), \tag{1}$$

where $\sigma(t)$ is the time-dependent sample photoconductivity and τ is relaxation time. We calculated τ by a mathematical procedure performed on the experimental data such that $\tau = -1/(dln\sigma(t)/dt)$. The values obtained for τ are 22.4 and 17.1 h for undoped *p*-PbTe and *p*-PbTe:BaF_2, respectively, at room temperature. The higher variation of σ_N observed for the doped sample can be related to its lower hole concentration (see Table I). On the other hand, the recombination time for *p*-PbTe:BaF_2 is lower than the value found for *p*-PbTe. This could be caused due to the presence of inhomogeneities originated from the BaF_2 doping that increases the scattering and reduces the mobility (see Table I) leading to a faster recombination.

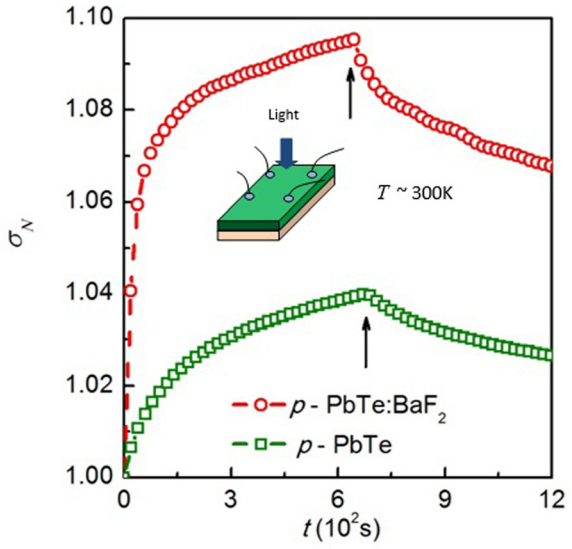

FIG. 1. Photoconductivity normalized (σ_N) at $t = 0$ under illumination by blue LED for undoped *p*-PbTe sample (open square) and *p*-PbTe:BaF_2 (open circles) at 300 K. The arrows indicate the moment of switching off illumination. Both samples exhibit PPC effect after switch off the light.

Figure 2 shows the time dependence of the σ_N measurement for temperatures of 300, 230, 190, 170, 150, 130, and 100 K for *p*-PbTe:BaF_2 sample. Figure 2(a) exhibits σ_N when the excitation light from the blue LED is turned on with perpendicular illumination. σ_N increases and its amplitude scales with temperature. In Figure 2(b), after the excitation light is turned off, σ_N slowly decreases and continue decreasing for hours, showing PPC at all temperatures measured. For temperatures below 100 K, the measured films showed no photoconductivity effect.

In order to elucidate the origin the PPC effect and the profiles observed in Figure 2, we obtained the recombination times using Eq. (1) for each temperature measured. The temperature dependence of the recombination time is illustrated in Figure 3(a) for doped (open squares) and undoped (open circles) *p*-PbTe films. For the doped sample, it is possible to observe that the recombination time increases as temperature decreases from 300 K down to 150 K but starts to decrease as temperatures decreases bellow 150 K clearly indicating a transition around 150 K. For the undoped sample, the recombination time increases as temperature decreases from 300 K down to 235 K. For temperatures lower than 235 K, there is no photoresponse (see inset).

For processes in which trapped electrons or holes are thermally freed from traps to the bands, the temperature dependence of τ can be expressed by[21]

$$\frac{1}{\tau} = N_c \beta_n \exp\left(-\frac{\Delta E}{k_B T}\right), \tag{2}$$

where N_c is the density of states in the conduction band, β_n is the capture coefficient of traps for electrons, ΔE is the trap depth or ionization energy, and k_B is the Boltzmann constant. The fittings using Eq. (2) are also presented in Figure 3(a) (dashed lines) and the trap energies obtained for the doped sample are $\Delta E_1 \sim 62$ meV and $\Delta E_2 \sim 12$ meV for $T > 150$ K and $T < 150$ K, respectively. For the undoped sample, the obtained energy is $\Delta E \sim 35$ meV. Theoretically, the energy barrier responsible for the increase of τ is due to a potential relief, generally associated with random inhomogeneities, and can be calculated by[16]

$$E_t = \frac{e^2 N^{2/3}}{\varepsilon n_0^{1/3}}, \tag{3}$$

where N is the impurity density, n_o is the density of charge carriers, and ε is the dielectric constant. The temperature dependence of the dielectric constant for PbTe can be calculated using the Barrett expression $\varepsilon = M/[0.5T_1 \coth(T_1/2T) - T_0]$,[21] where $M = 1.5 \times 10^5$, $T_1 = 410$ K, and $T_0 = 1$ K. Hence, one can derive de values of E_t. We take an average between 150

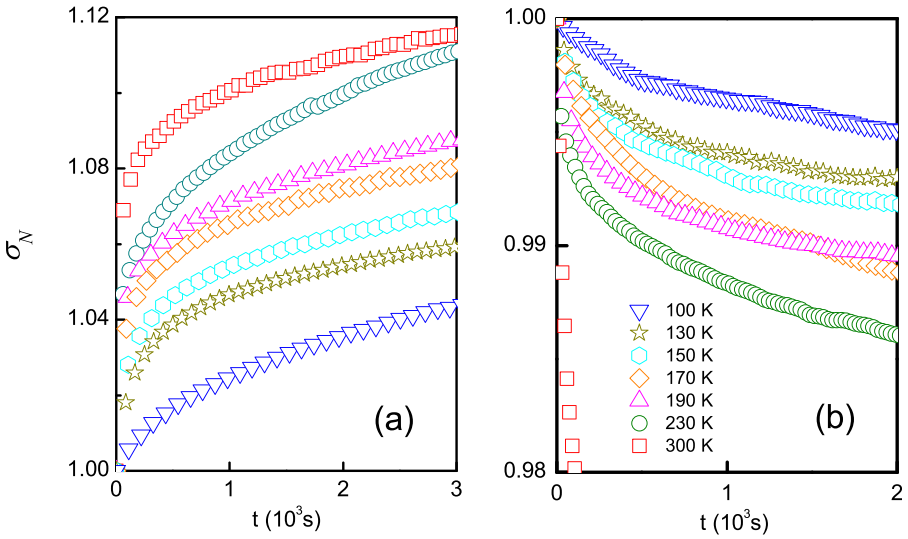

FIG. 2. Time dependence of the normalized photoconductivity when (a) turned on and (b) turned off the blue LED for temperature range $T = 100$–300 K. The sample exhibits persistent photoconductivity in all temperatures measurements.

and 300 K and we obtained $E_t \sim 24$ meV, which has a difference of ~38 meV from the experimental value ΔE_1(~62 meV) found for the doped sample. This suggests the existence of an additional energy barrier, $\Delta E_3 \sim 38$ meV, which cannot be described by the model in this temperature range. The existence of the barrier with energy height ΔE_3 is probably due to intrinsic disorder present in *p*-PbTe sample, i.e., Te vacancies, which explains why the persistent photoconductivity is also present in undoped *p*-PbTe sample as observed in Figure 1. In fact, for the undoped sample, the obtained value ($\Delta E \sim 35$ meV) is very close to ΔE_3. On the other hand, for the temperature range of $T = 100$–150 K, the value of E_t approaches to ΔE_2. Figure 3(b) presents a comparison of the energies ΔE_2, ΔE_3, E_t, and k_BT. ΔE_1 is not plotted in this graphic and was considered as $\Delta E_1 = E_t + \Delta E_3$. Even though E_t is temperature dependent, the constant values of ΔE_2 and ΔE_3 indicate the effective trap barrier in each temperature region. Through this figure, it is also possible to observe that the thermal energy crosses ΔE_2 around $T \sim 150$ K. This means that for $T > 150$ K, the trapping due to ΔE_2 is weak and can be neglected. For such temperatures, ΔE_3 is the main responsible for trapping the hole carriers since $k_BT < \Delta E_3$. In addition, for $T < 150$ K, when ΔE_2 becomes more effective, ΔE_3 unexpectedly ceases to participate in the trapping process. It is possible that ΔE_3 is located in the Γ point in the Brillouin zone and the phonons energy ($\hbar\omega$) for $T < 150$ K is not enough to transfer the holes to this point in *k* space.[22–24] Hence, for temperatures below 150 K, holes are no longer transferred to other point in *k* space remaining in the *L* point of Brillouin zone, causing a redistribution of the holes through the valence band. This enables the electrons previously photo excited to the conduction band to recombine back in the valence band causing the decrease of the recombination time and the negative slope of −12 meV observed in Figure 3(a). Similar behavior was observed for C_{60} single crystals, where an inversion of the slope sign for recombination time temperature dependence was also observed due to re-distribution of hole carriers.[25] For the undoped sample, since there is no trapping level due to BaF_2 doping, the persistent photoconductivity must vanish for low temperatures which is in agreement with the experimental data observed in Figure 3(a).

Figure 4 is a pictorial representation of the analysis discussed above. The vertical arrows represent the possible transitions in the band structure taking into account the LED energy. The open and dark circles represent the holes and electrons, respectively. The horizontal arrow represents the possible phonon interaction that promotes holes to other point in the Brillouin zone where they can be trapped

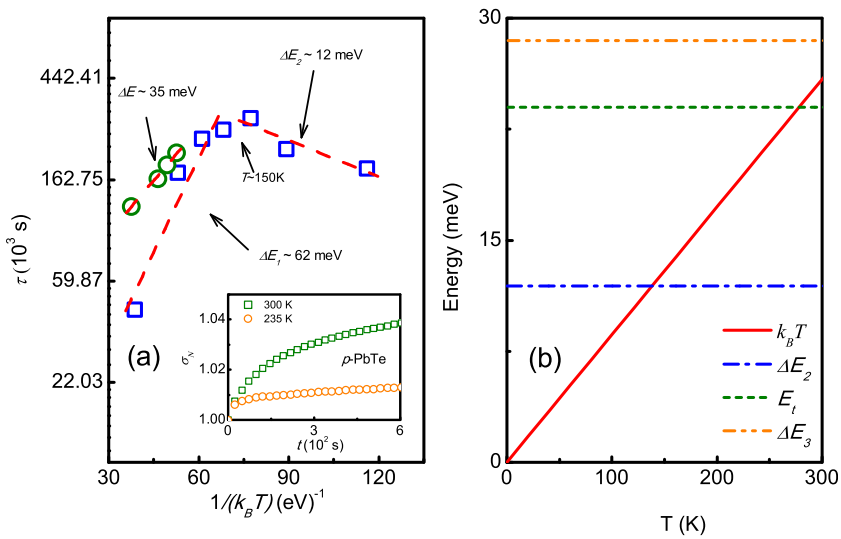

FIG. 3. (a) Arrhenius plot for *p*-PbTe:BaF_2 and *p*-PbTe. The inset shows the photoconductivity for *p*-PbTe at 300 K and 235 K. (b) Comparing ΔE_1, ΔE_2, and ΔE_3 with thermal energy k_BT and E_t.

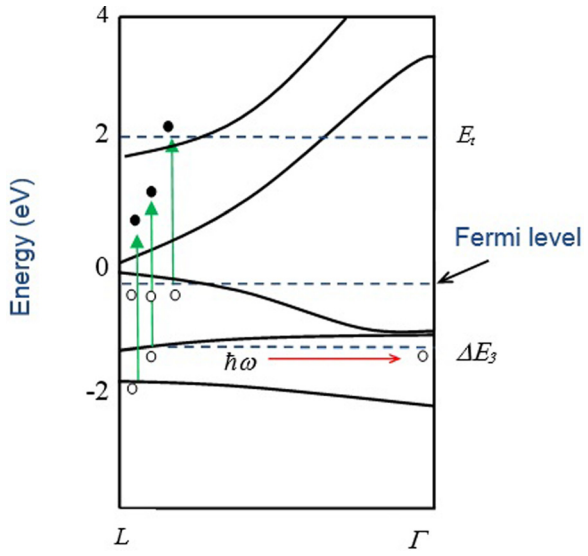

FIG. 4. Pictorial representation of the photo-excitation. Open and dark circles represent the holes and electrons, respectively. The vertical arrows represent the possible transitions in the band structure and the horizontal one represents the possible phonon interaction that promotes holes through energy barrier ΔE_3. The barrier energy caused by random inhomogeneities E_t is also indicated. This region is actually a region of localized states and depends on the BaF_2 doping.

through energy barrier ΔE_3. The Fermi energy is also indicated and it is resonant to the valence band.[17] The barrier energy caused by random inhomogeneities E_t is also indicated and is located inside the band above 2 eV according to the LED energy, i.e., for LED's with low energy, no photoresponse at room temperature is observed.[10] This region is actually a region of localized states and depends on the BaF_2 doping. Once hole carrier are trapped in these regions, the PPC effect manifests in these samples.

In conclusion, we have investigated the PPC effect observed on undoped *p*-PbTe and *p*-PbTe:BaF_2 samples. We used the random potential model to analyze the experimental data and we found that the hole carriers are trapped in two different energy barriers and each barrier is more effective depending on the temperature region. The description of the PPC effect in PbTe:BaF_2 makes possible a better understanding of the physics involved in such systems under illumination. In addition, the obtained relaxation times are the order of hours and, in some cases, days, revealing the potential of application of this material on the development of holographic memories.

We would like to thank CAPES for financial support.

[1]D. E. Theodorou and E. A. Anagnostakis, Phys. Rev. B **44**, 3352 (1991).
[2]E. Arslan, S. Bütün, S. B. Lisesivdin, M. Kasap, S. Ozcelik, and E. Ozbay, J. Appl. Phys. **103**, 103701 (2008).
[3]K. Sieranski, J. Szatkowski, and J. M. Pawlikowski, J. Appl. Phys. **115**, 083709 (2014).
[4]J. C. González, G. M. Ribeiro, E. R. Viana, P. A. Fernandes, P. M. P. Salomé, K. Guitiérrez, A. Abelenda, F. M. Matinaga, J. P. Leitão, and A. F. da Cunha, J. Phys. D: Appl. Phys. **46**, 155107 (2013).
[5]H. M. Chen, Y. F. Chen, M. C. Lee, and M. S. Feng, J. Appl. Phys. **82**, 899 (1997).
[6]C. Johnson, J. Y. Lin, H. X. Jiang, M. Asif Khan, and C. J. Sun, Appl. Phys. Lett. **68**, 1808 (1996).
[7]L. H. Chu, Y. F. Chen, D. C. Chang, and C. Y. Chang, J. Phys.: Condens. Matter. **7**, 4525 (1995).
[8]M. C. Tarun, F. A. Selim, and M. D. McCluskey, Phys. Rev. Lett. **111**, 187403 (2013).
[9]B. A. Akimov, V. A. Bogoyavlenskiy, L. I. Ryabova, and V. 'N. Vasil'kov, Phys. Rev. **61**, 16045 (2000).
[10]M. H. Maksimov, L. V. Vassilev, Yu. G. Besedin, and T. Dyakov, Infrared Phys. **31**, 199 (1991).
[11]J. John and H. Zogg, J. Appl. Phys. **85**, 3364 (1999).
[12]H. W. L. Alves, A. R. R. Neto, L. M. R. Scolfaro, T. H. Myers, and P. D. Borges, Phys. Rev. B **87**, 115204 (2013).
[13]A. Rogalski, Infrared Phys. Technol. **43**, 187 (2002).
[14]D. Khokhlov, *Lead Chalcogenides* (Tayler & Francis Books, Inc., 2003).
[15]G. Grabecki, J. Appl. Phys. **101**, 081722 (2007).
[16]A. Ya. Shik, Sov. Phys. JETP **41**, 932 (1975), available at http://www.jetp.ac.ru/cgi-bin/e/index/e/41/5/p932?a=list.
[17]U. A. Mengui, E. Abramof, P. H. O. Rappl, B. Díaz, H. Closs, J. R. Senna, and A. Y. Ueta, J. Appl. Phys. **105**, 043709 (2009).
[18]G. Nimtz, Phys. Rep. **63**, 265 (1980).
[19]B. A. Volkov, L. I. Ryabova, and D. R. Khokhlov, Phys.-Usp. **45**, 819 (2002).
[20]R. H. Bube, *Photoelectronic Properties of Semiconductors* (Cambridge University Press, New York, 1992).
[21]J. H. Barrett, Phys. Rev. **86**, 118 (1952).
[22]H. J. Queisser and D. E. Theodorou, Phys. Rev. B **33**, 4027 (1986).
[23]G. W. Iseler, J. A. Kafalas, and A. J. Strauss, Solid State Commun. **10**, 619 (1972).
[24]K. A. Baklanov and I. P. Kryolov, Sov. Phys. JETP **74**, 157 (1992), available at http://www.jetp.ac.ru/cgi-bin/e/index/r/101/1/p294?a=list.
[25]K. C. Chiu, J. S. Wang, Y. T. Dai, and Y. F. Chen, Appl. Phys. Lett. **69**, 2665 (1996).